# $[(MeCN)Ni(CF_3)_3]^{1-}$ and $[Ni(CF_3)_4]^{2-}$ : Foundations Towards the Development of Trifluoromethylations at Unsupported Nickel

Scott T. Shreiber,[†] Ida M. DiMucci,[‡] Mikhail N. Khrizanforov,[ξ] Charles J. Titus,[℘] Dennis Nordlund,[ℵ] Yulia Dudkina, [ξ]Roger E. Cramer,[ζ] Yulia Budnikova,[ξ] Kyle M. Lancaster,[‡*] and David A. Vicic[†*]

[†]Department of Chemistry, Lehigh University, 6 E Packer Ave., Bethlehem, PA 18015.

[‡]Department of Chemistry and Chemical Biology, Baker Laboratory, Cornell University, Ithaca, NY 14853, USA

[℘]Department of Physics, Stanford University, Stanford, California 94305, USA

[ℵ]Stanford Synchrotron Radiation Lightsource, SLAC National Accelerator Laboratory, Menlo Park, California 94025, USA

[ζ]Department of Chemistry, University of Hawaii, 2545 McCarthy Mall, Honolulu, HI, 96822, USA

[ξ]A.E. Arbuzov Institute of Organic and Physical Chemistry, Kazan Scientific Center of Russian Academy of Sciences, 8, Arbuzov Str., 420088 Kazan, Russian Federation

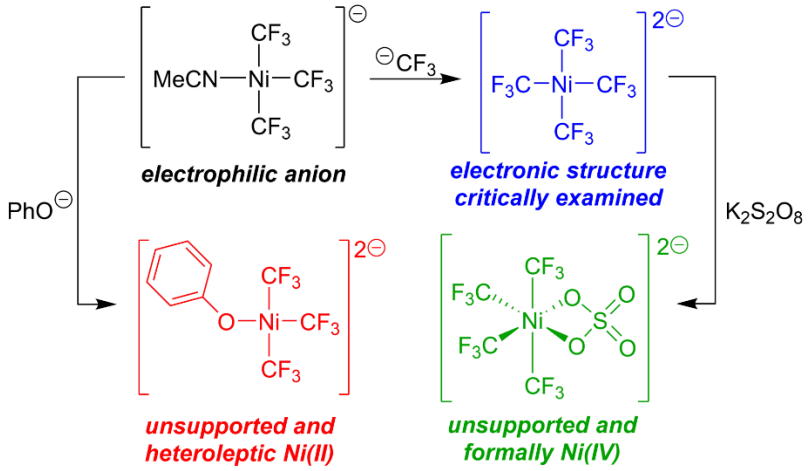


**Abstract:** The nickel anions $[(MeCN)Ni(CF_3)_3]^{1-}$ and $[Ni(CF_3)_4]^{2-}$ were prepared by formal addition of three and four equivalents of $[AgCF_3]$ to $[(dme)NiBr_2]$ in the presence of supporting $[PPh_4]$ counter-ion. Detailed insights into the electronic properties of these new compounds were obtained through the use of density functional theory (DFT) calculations, spectroscopy-oriented configuration interaction (SORCI) calculations, X-ray absorption spectroscopy, and cyclic voltammetry. The data collectively show that trifluoromethyl complexes of nickel, even in the most common oxidation state of nickel(II), are highly covalent systems whereby a hole is distributed on the trifluoromethyl ligands and surprisingly rendering the metal to a physically more reduced state. In the cases of $[(MeCN)Ni(CF_3)_3]^{1-}$ and $[Ni(CF_3)_4]^{2-}$, these complexes are better described as physically $d^9$ metal complexes. $[(MeCN)Ni(CF_3)_3]^{1-}$ is electrophilic and reacts with other nucleophiles like phenoxide to yield the unsupported $[(PhO)Ni(CF_3)_3]^{2-}$ salt, revealing the broader potential of $[(MeCN)Ni(CF_3)_3]^{1-}$ in the development of ligandless trifluoromethylations at nickel. Proof-in-principle experiments show that reaction of $[(MeCN)Ni(CF_3)_3]^{1-}$ with an aryl iodonium salt yields trifluoromethylated arene, presumably via a high valent, unsupported, and formally organonickel(IV) intermediate. Evidence for the feasibility of such intermediates is provided with the structurally characterized $[Ni(CF_3)_4(SO_4)][PPh_4]_2$, which was derived through the two electron oxidation of $[Ni(CF_3)_4]^{2-}$.

**Introduction**

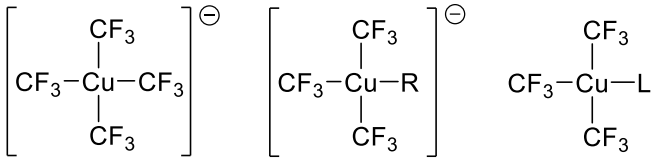

**1** **2** **3**

It was first reported (without full experimental disclosure)[1] that the complex ion $[Cu(CF_3)_4]^-$ (**1**) could be generated by the oxidation of the cuprate salt $[Cu(CF_3)_2]^-$. Shortly thereafter, Naumann and co-workers reported the synthesis and isolation of $[Cu(CF_3)_4][PPh_4]$ as well as the X-ray structure of the related salt $[Cu(CF_3)_4][PPN]$.[2] The $[Cu(CF_3)_4]^-$ core was described as having "surprising"[2] stability as it possessed a rare and formally copper(III) center. Knowledge of the structure of **1** stimulated studies of its electronic structure, and in 1995 Snyder put forth the provocative analysis that the trifluoromethyl ligands were oxidized rather than the copper center (a feature later referred to as "sigma non-innocence"[3-4]) and that the oxidation state of the copper ion in **1** was actually copper(I) and not copper(III).[5] Such a description of the electronic state of **1** has sparked debate and further theoretical studies,[3, 6-7] but recent experimental evidence for a $3d^{10}$ ground state electronic configuration and ligand field inversion in **1**[8-10] supports Snyder's original proposal of a copper(I) complex that displays sigma non-innocence of the trifluoromethyl ligands.

Salts of **1** have not only been important for providing insights into the nature of bonding in metal-fluoroalkyl complexes, but have also demonstrated reactivity important to the development of trifluoromethylation methodologies. For example, Zhang and co-workers revealed that equilibria involving ion pairs of $[Cu(CF_3)_4]^-$ can be exploited in reactions with aryl boronic acids to afford high yields of trifluoromethylated arenes (Scheme 1a).[11] Menjon and co-workers showed that **1** can generate trifluoromethyl radicals under photolytic conditions which could then be trapped by arenes and nitrones (Scheme 1b).[12] Importantly, the homoleptic tetra(trifluoromethyl)copper(III) functionality in **1** can also be rendered into heteroleptic derivatives (**2**) by addition of nucleophiles to charge-neutral tris(trifluoromethyl)copper complexes (**3**, Scheme 1c). This derivatization is of high synthetic value as eliminations from **2** can render cross-coupled and trifluoromethylated organic products.[13-14] Finally, the charge-neutral tris(trifluoromethyl)copper derivatives **3** have also served as precursors of $[LCu(CF_3)_2(R)]$[15-18] intermediates *en route* to the generation of $[R\text{-}CF_3]$ products (Scheme 1d).

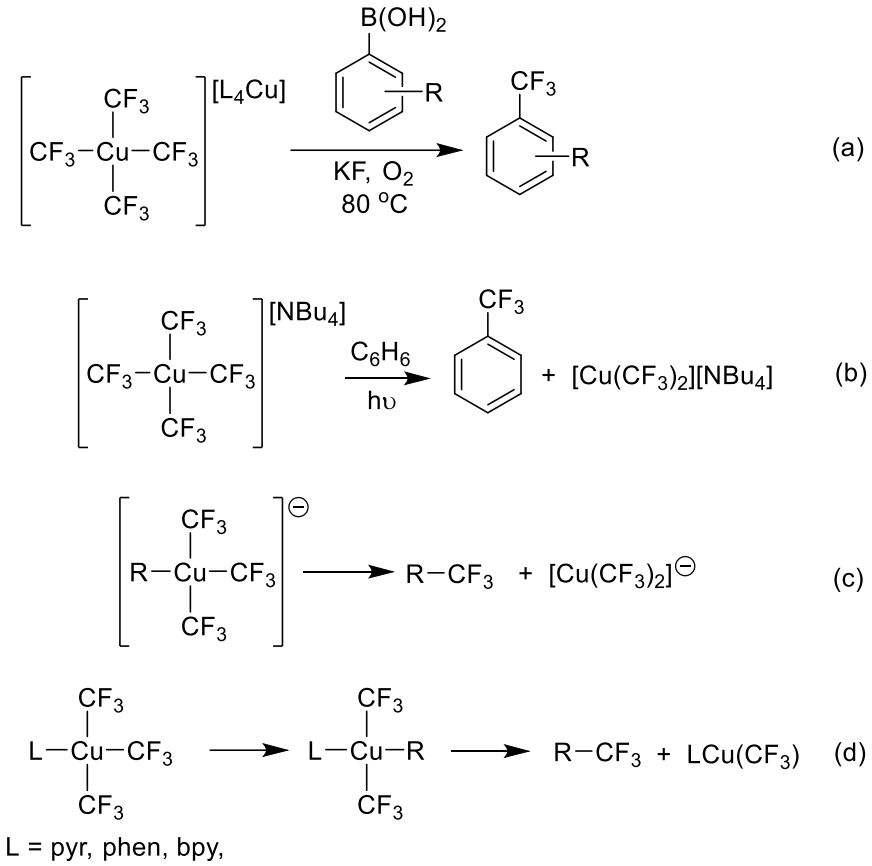


**Scheme 1.** Known applications of formally copper(III) trifluoromethyl copper complexes.

We hypothesized that a homoleptic tetra(trifluoromethyl)metal complex bearing a bona fide $d^8$ ground state electronic configuration may be possible with nickel, as nickel in the +2 oxidation state is more commonly encountered than copper in its +3 oxidation state. Moreover, if $[Ni(CF_3)_4]^{2-}$ and $[Ni(R)(CF_3)_3]^{2-}$ complexes could be generated, then access to their higher oxidation states would be more facile than for $[Cu(CF_3)_4]^{1-}$ and $[LCu(CF_3)_2(R)]$ derivatives, which are already highly oxidized molecular species. Nickel fluoroalkyl complexes often exhibit two additional oxidations beyond the formal nickel(II) state and show higher reactivity in their oxidized forms.[19-22] Access to higher oxidation states would provide the opportunity to explore whether difficult chemical bond forming reactions involving the trifluoromethyl group could be triggered by oxidative means with "ligandless" (unsupported) architectures at nickel.

**Results and Discussion**

*Synthesis.*

A family of trifluoromethyl nickel complexes could be prepared by routes that all employ a common set of starting materials and reagents, as described in Scheme 2. It is known that reaction of [(dme)$NiBr_2$] with two equivalents of [$Me_3Si$-$CF_3$] and [AgF] leads to the charge neutral (bis)trifluoromethyl complex **4**.[23] Here, we reveal that reaction of [(dme)$NiBr_2$] with an extra equivalent of [$Me_3Si$–$CF_3$] and [AgF] in the presence of [$PPh_4$]Cl in acetonitrile cleanly leads to the formation of the new anionic tris trifluoromethyl complex **5** in 93% yield. Diagnostic $^{19}F$ NMR signals for **5** arise from the two types of trifluoromethyl groups situated in a static and square planar arrangement ($CD_3CN$, δ –25.23 (septet, *J* = 4.5 Hz, 3F) and –31.06 (quartet, *J* = 4.5 Hz, 6F)). Gratifyingly, performing the trifluoromethylation of [(dme)$NiBr_2$] with slightly over 4 equivalents of [$Me_3Si$-$CF_3$] and [AgF] in the presence of [$PPh_4$]Cl leads to the appearance of a new singlet in the $^{19}F$ NMR at δ –26.24 that corresponds to the target dianionic complex **6**. Complete conversion to **6** was difficult to achieve, but the solubility properties of the dianion facilitated its isolation in analytically pure form in 19% yield.

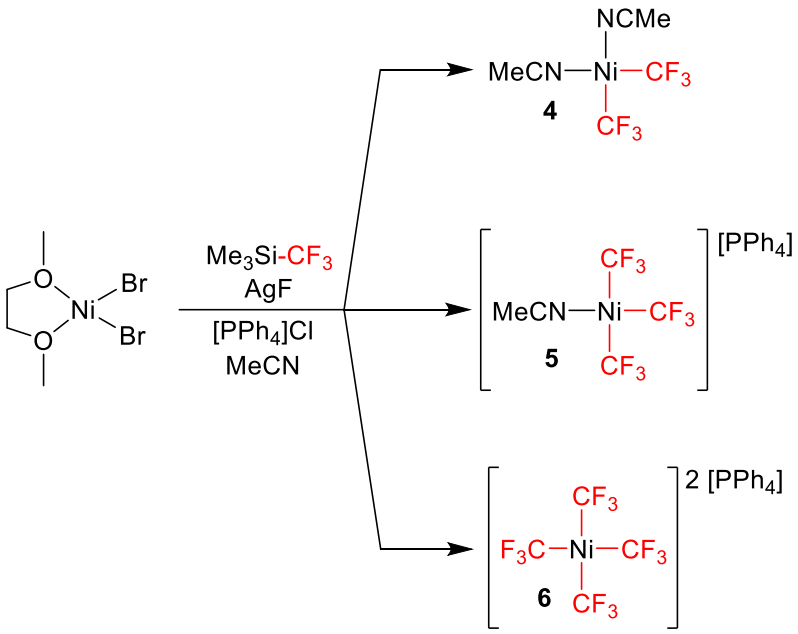


**Scheme 2.** Generation of "ligandless" trifluoromethyl complexes of nickel from a common starting material.

The structures of the new complexes **5** and **6** were confirmed by X-ray crystallography, and ORTEP diagrams of both structures are shown in Figure 1. Rotational disorders of the trifluoromethyl groups in **5** prevented rigorous quantitative analysis of the crystallographic bond lengths and angles, but it is clear that the nickel centers of both structures adopt a distorted square planar geometry, with complex **6** showing a slightly larger distortion which is highlighted in the side-on view of **6** in Figure 1. The *trans* trifluoromethyl groups in **5** are situated at an angle of 177.90(10)° while the *trans* trifluoromethyl groups at **6** have angles of 168.10(17) and 166.49(17)°. For reference, the angles for the *trans* trifluoromethyl ligands in $[Cu(CF_3)_4]^-$ were measured at 165.0(7) and 172.2(6)°.[2]

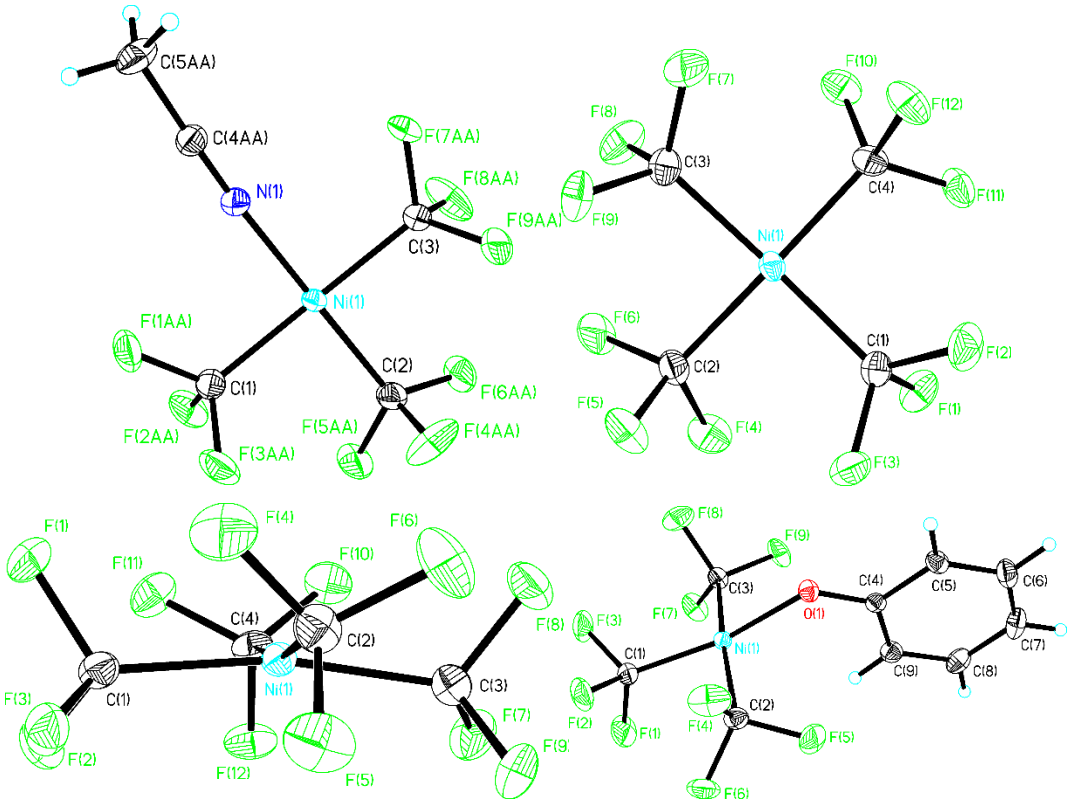


**Figure 1.** ORTEP diagrams of the nickel centers of **5** (top left), **6** (top right and bottom left), and **7** (bottom right). Selected bond lengths (Å) for **5**: Ni1-N1 1.8816(18); Ni1-C2 1.885(2); Ni1-C3 1.938(2); Ni1-C1 1.953(2). Selected bond angles (°) for **5**: N1-Ni1-C2 177.62(10); N1-Ni1-C3 89.43(8); C2-Ni1-C3 90.15(9); N1-Ni1-C1 90.28(8); C2-Ni1-C1 90.06(9); C3-Ni1-C1 177.90(10). Selected bond lengths (Å) for **6**: Ni1-C4 1.924(4); Ni1-C3 1.927(4); Ni1-C1 1.930(4); Ni1-C2 1.939(4). Selected bond angles (°) for **6**: C4-Ni1-C3 90.40(17); C4-Ni1-C1 91.82(17); C3-Ni1-C1 168.10(17); C4-Ni1-C2 166.49(17); C3-Ni1-C2 89.89(18); C1-Ni1-C2 90.66(17). Selected bond lengths (Å) for **7**: Ni1 C1 1.8989(13); Ni1-O1 1.9056(9); Ni1-C2 1.9342(13); Ni1-C3 1.9448(13). Selected bond angles (°) for **7**: C1-Ni1-O1 165.64(5); C1-Ni1-C2

90.16(6); O1-Ni1-C2 89.08(5); C1-Ni1-C3 91.62(6); O1-Ni1-C3 91.06(5); C2-Ni1-C3 172.23(6); C4-O1-Ni1 128.35(8).

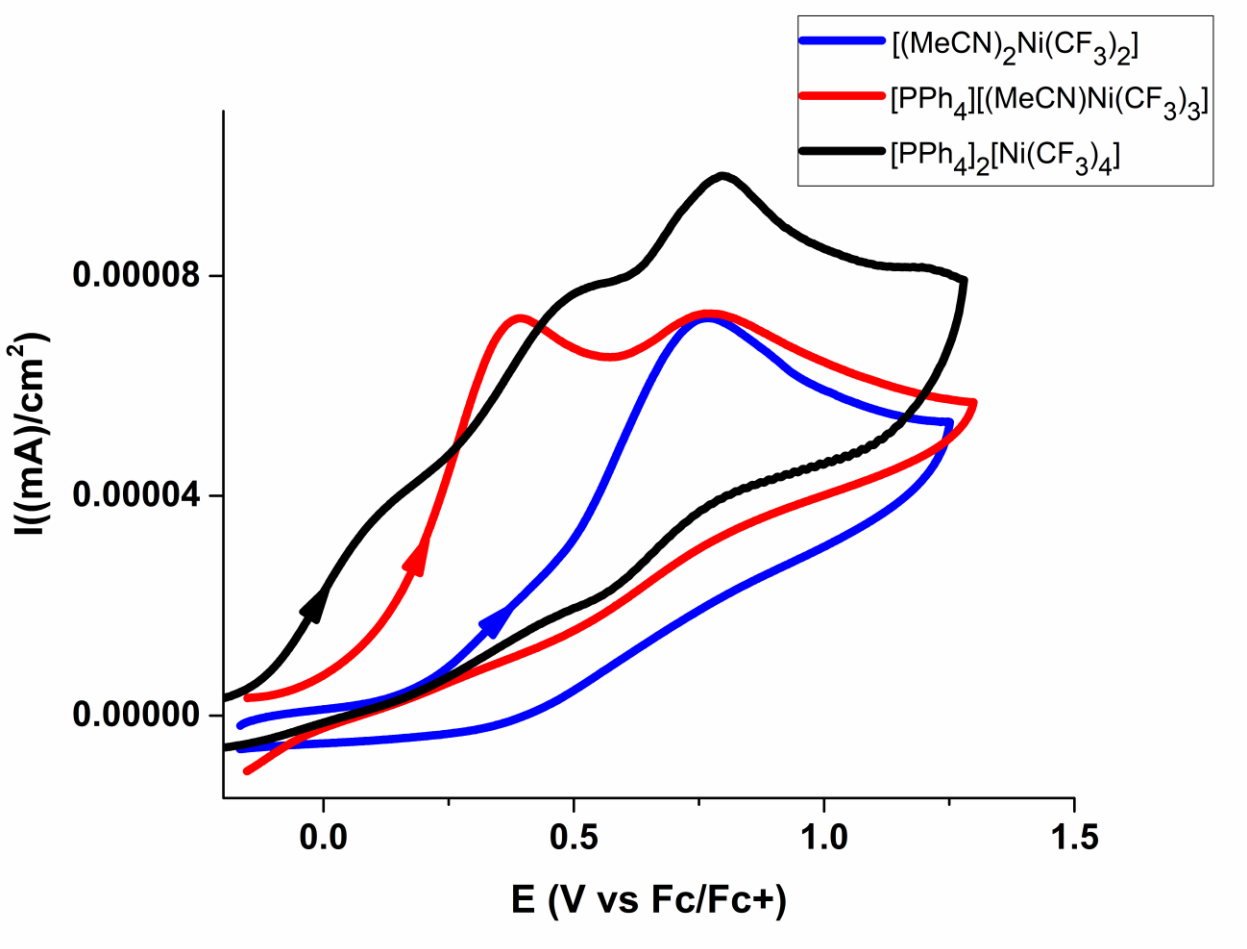


**Figure 2.** Cyclic voltammograms of **4** (blue), **5** (red), and **6** (black) in MeCN. Metal complex: 0.5 mM. Electrolyte: $[Bu_4N][PF_6]$ (100 mM); working electrode: glassy carbon; counter electrode: platinum. Scan rate: 100 mV/s.

*Electrochemistry.*

With complexes **5** and **6** in hand, we evaluated their electrochemical properties by cyclic voltammetry (Figure 2). Oxidation of the monoanionic $[(MeCN)Ni(CF_3)_3][PPh_4]$ is irreversible and occurs at the onset potential of ca. +0.02 V vs the ferrocene/ferrocenium couple. Peak potentials for **5** appear at +0.38 V and +0.76 V. The oxidation of complex **6** was more facile, with an onset potential of ca. -0.1 V and peak potentials at +0.10, +0.50 and +0.79 V. Interestingly, both **5** and **6** display peak potentials in the region where oxidation occurs for the bis-trifluoromethyl complex **4** (Figure 2), suggestive that upon oxidation **5** and **6** undergo chemical transformations leading to **4**. However, since the waves in the CVs are all

irreversible, more evidence will be required corroborate this speculation. The CVs are interesting to compare with that of the copper derivative $[Cu(CF_3)_4][NBu_4]$ ([**1**][$NBu_4$]). Because [**1**][$NBu_4$] is already a highly oxidized species (irrespective of whether the holes lie predominantly on the metal or ligand), no oxidation peak was observed in the CV in the region spanning from 0 to +1.5 V vs the ferrocene/ferrocenium couple (see Supporting Information). Thus, changing the metal identity from copper to nickel in the $[M(CF_3)_4]^{n-}$ (and formally $d^8$) platform provides exciting opportunities to explore redox triggered-reactions involving this ligandless trifluoromethyl source using readily available and practical oxidants.

*UV/Visible and Multi-Edge X-Ray Absorption Spectroscopy.*

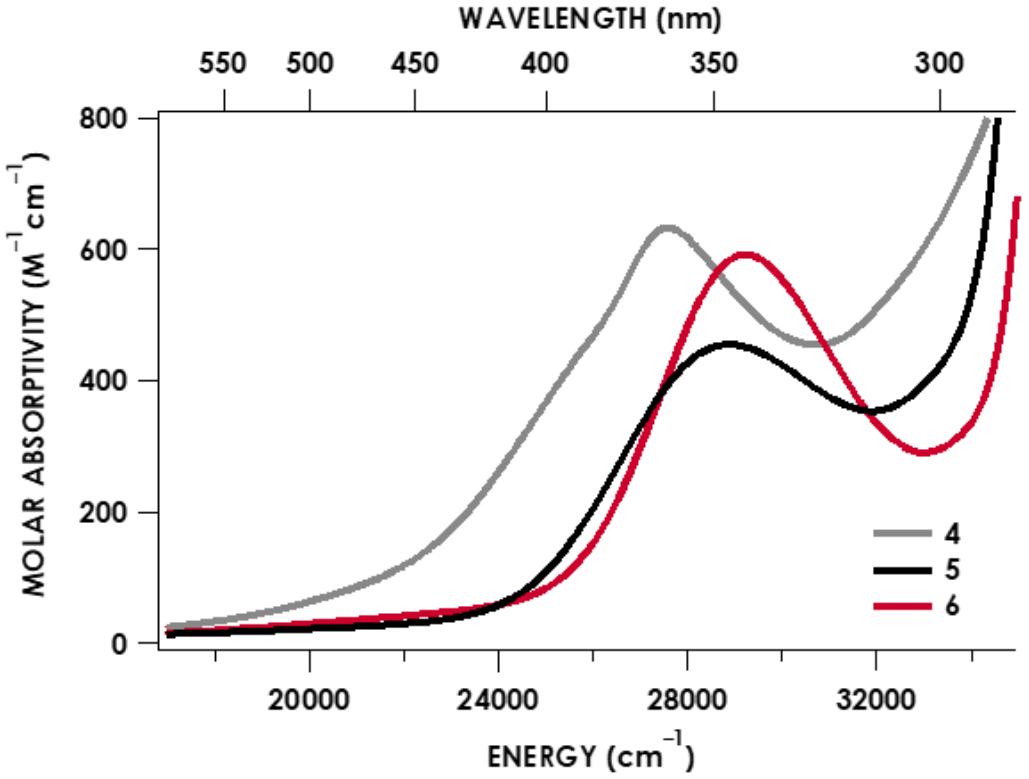


**Figure 3.** Room-temperature UV/visible absorption spectra of compounds **4**-**6** dissolved in MeCN.

UV/visible absorption spectra obtained for **4**–**6** are shown in Figure 3. Each complex shows a broad absorbance with $\lambda_{max}$ ca. 350 nm (28500 $cm^{-1}$). These bands have modest absorptivities ca. 600 $M^{-1}cm^{-1}$, reasonably within the range expected for a d-d band for a nickel center with $D_{2d}$ symmetry. By contrast, the UV/visible absorption spectrum of salts of **1** exhibit a broad absorption band at 270 nm (36900 $cm^{-1}$) with an extinction coefficient of 21,550 $M^{-1}cm^{-1}$. The assignment of this band in **1** to a ligand-ligand charge-transfer transition was supported by both time-dependent DFT (TDDFT) and (SORCI) calculations.[8]

Ni K-edge (1s $\rightarrow$ valence/continuum) XAS data were obtained for compounds **5** and **6**. The spectra each feature a well-resolved, intense pre-edge transition that have maxima at 8335.2 and 8335.4 eV, respectively, consistent with Ni 1s $\rightarrow$ 4p excitations. Both features exhibit shoulders with maxima at 8332.5 and 8332.7 eV (for **5** and **6**, respectively). Features in this energy and intensity range are conventionally assigned as Ni 1s $\rightarrow$ 3d excitations, although such features also arise due to excitations to acceptor MOs dominated by ligand character. The Cu K-edge XAS of **1** presents a qualitatively similar spectrum with a well-resolved 1s $\rightarrow$ 4p transition and intense peak to lower energy assigned as the Cu 1s $\rightarrow$ LUMO.[8] The rising edge inflection points in the Ni K-edges of **5** and **6** occur at 8345.6 and 8346.2 eV, respectively. This shift is plausibly attributable to the change in coordination upon substitution of N-donor MeCN for C-donor $CF_3^-$.

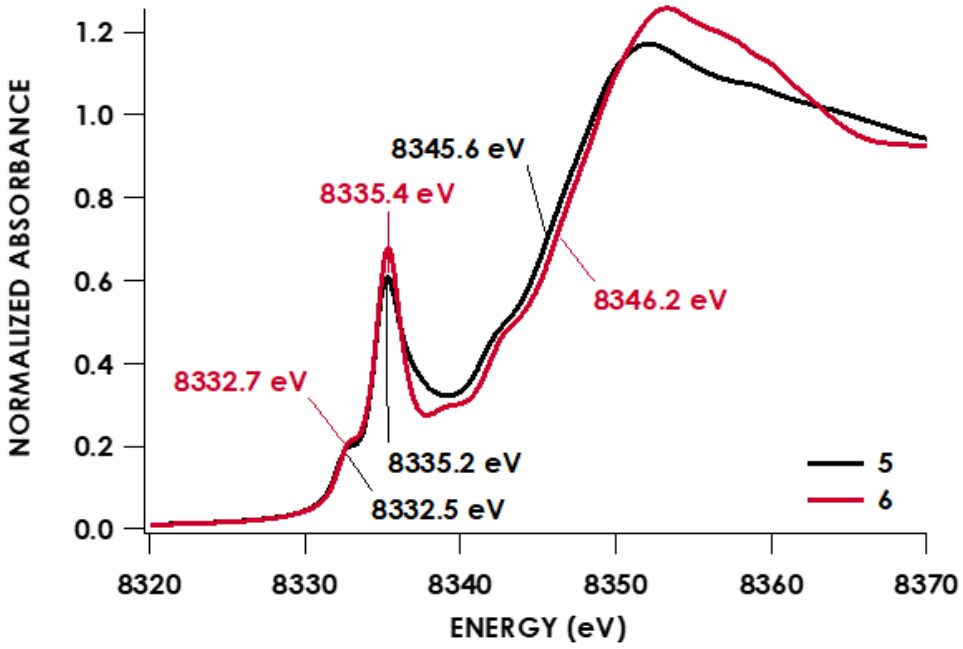


**Figure 4.** Ni K-edge XAS data obtained for **5** (black) and **6** (red). Compounds were measured as solids diluted in boron nitride (BN) and maintained at 10 K, with data were obtained in fluorescence mode using a PIPS (passivated, implanted, planar silicon) detector. Pre-edge peak positions were determined from second derivatives, while the rising edge inflection points were determined via first derivatives.

Ni $L_{2,3}$-edge (2p → valence/continuum) XAS data were obtained for **5** and **6** (Figure 5a). Ni 2p → 3d excitations are dipole allowed and thus intense, but lose intensity commensurate with ligand orbital admixture into 3d-containing frontier MOs. Consequently, total $L_{2,3}$-edge XAS areas afford a convenient means to quantify 3d participation in vacant MOs. The splitting between the $L_3$ and $L_2$ peaks arises due to 2p spin-orbit coupling. The $L_3$ peaks for **5** and **6** occur at 854.3 and 854.4 eV, respectively. The $L_2$ peaks for **5** and **6** occur at 871.1 and 871.3 eV, respectively. For comparison, typical low-spin $Ni^{II}$ species show $L_3$ peaks at 853.3 ± 0.5 and $L_2$ at 870.4 ± 0.5 eV.[24-25] This shift in $L_{2,3}$-edge is consistent with what was seen when comparing **1** to other $Cu^{II}$ species in the literature, and not necessarily indicative of metal oxidation. Errors in $L_{2,3}$-edge areas are estimated at 10%. These errors are estimated from uncertainties in peak fitting as well as saturation effects due to the high nickel concentration of the samples.[26] Saturation has been estimated using tabulated transmission coefficients for the background elements.[27] The saturation effect attenuates the partial-fluorescence yield-detected $L_{2,3}$-edge spectra by ca. 15% relative to the otherwise unobtainable transmission spectra, however because all spectra used in the analysis have a similar background absorption, the relative peak areas may be used to estimate Ni

covalency. Plots of $L_{2,3}$-edge spectra obtained via Ni 3s2p and 3d2p decay channels give superimposable spectra, indicating that self-absorption is not a source of error in the intensities (Figures S11-S12).[28] Using $(^nBu_4N)_2$ $[Ni(mnt)_2]$[29] and $(Et_4N)_2[NiCl_4]$[30] as covalency calibrants and assuming that 16-electron **5** and **6** have a single Ni 3d-containing LUMO, the total $L_{2,3}$-edge intensities give 48.9 ± 6.9 and 51.1 ± 7.1 % Ni 3d/hole for **5** and **6**, respectively (Figure 5b). This translates to Ni 3d vacancies of 1 electron—surprisingly, these complexes are more appropriately described as physically $d^9$ rather than $d^8$.

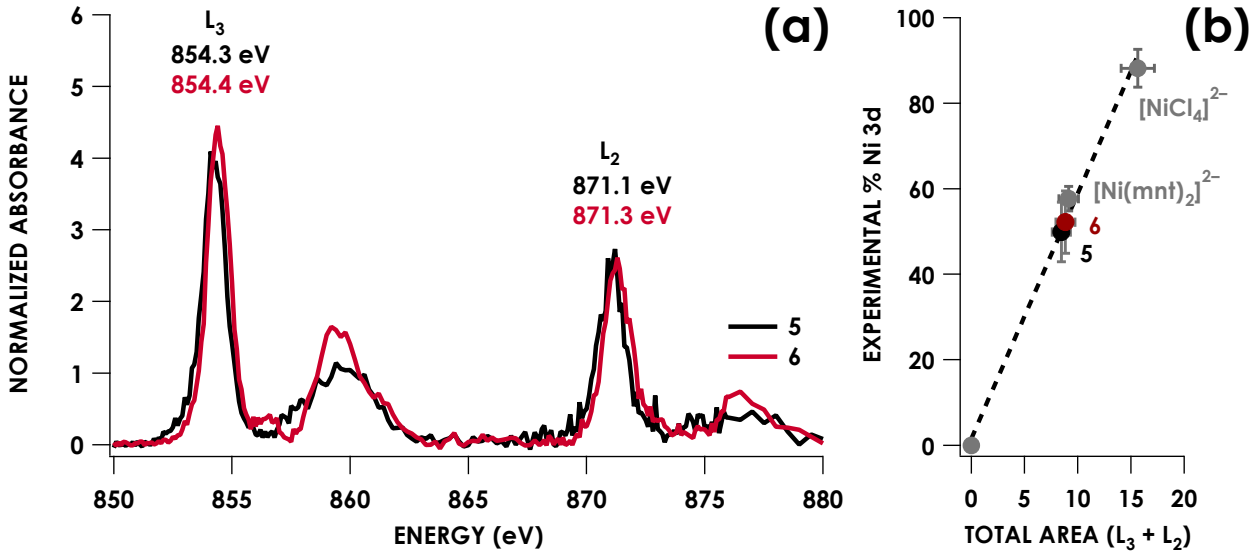


**Figure 5.** (a) Ni $L_{2,3}$-edge XAS obtained at 298 K from neat solid samples of **5** and **6**. Data were obtained via partial fluorescence yield detection windowed on Ni 3d → 2p X-ray emission. (b) Plot of Ni $L_{2,3}$ area vs. Ni 3d character. A line was fitted through zero and two calibrants with independently quantified Ni 3d covalencies yielding a line with slope = 5.69 ± 0.45 and y-intercept = 1.69 ± 4.71. The $R^2$ value is 0.994. The summed $L_{2,3}$ areas obtained for **5** and **6** are interpolated yielding 48.9 ± 6.9% and 51.1 ± 7.1% Ni 3d character per hole, respectively.

*Electronic Structure Calculations.*

Hybrid DFT calculations (B3LYP, CP(PPP) basis on Ni, ZORA-def2-TZVP(-f) on all other atoms) were carried out to investigate the electronic structures of **5** and **6**. These DFT single point calculations were used in subsequent time-dependent DFT calculations of the Ni K-edge XAS. Following conventional correction of the poorly-modeled Ni 1s core potential,[31] excellent agreement is obtained between calculated and experimental spectra. Scrutinizing the frontier MOs reveals the LUMO to be dominated

by Ni 4p character with only minor (ca. 15%) 3d participation. The LUMO + 1's are the expected Ni $3d_{x^2-y^2}$ orbital, but here the contribution of Ni 3d is only 35.7 % and 37.7 % for **5** and **6**, respectively. This is unexpected based on the K-edge XANES—the weaker shoulders near 8332 eV are consistent with an excitation to 3d, whereas the higher-energy, resolved peaks ca. 8335 eV have intensities consistent with Ni 1s $\rightarrow$ 4p. Scrutinizing the composition of the excited states, TDDFT predicts that both 1s $\rightarrow$ 4p and 1s $\rightarrow$ 3d excitations contribute to each pre-edge peak, with 1s $\rightarrow$ 3d dominating the ca 8332 eV pre-edge shoulders and 1s $\rightarrow$ 4p dominating the resolved 8335 eV peaks (Figure 6). Moreover, the averaged Ni 3d character distributed over four holes is 26.1% for **5** and 26.4 % for **6**, consistent with the $L_{2,3}$-edge intensities and supporting a ground state $d^9$ configuration.

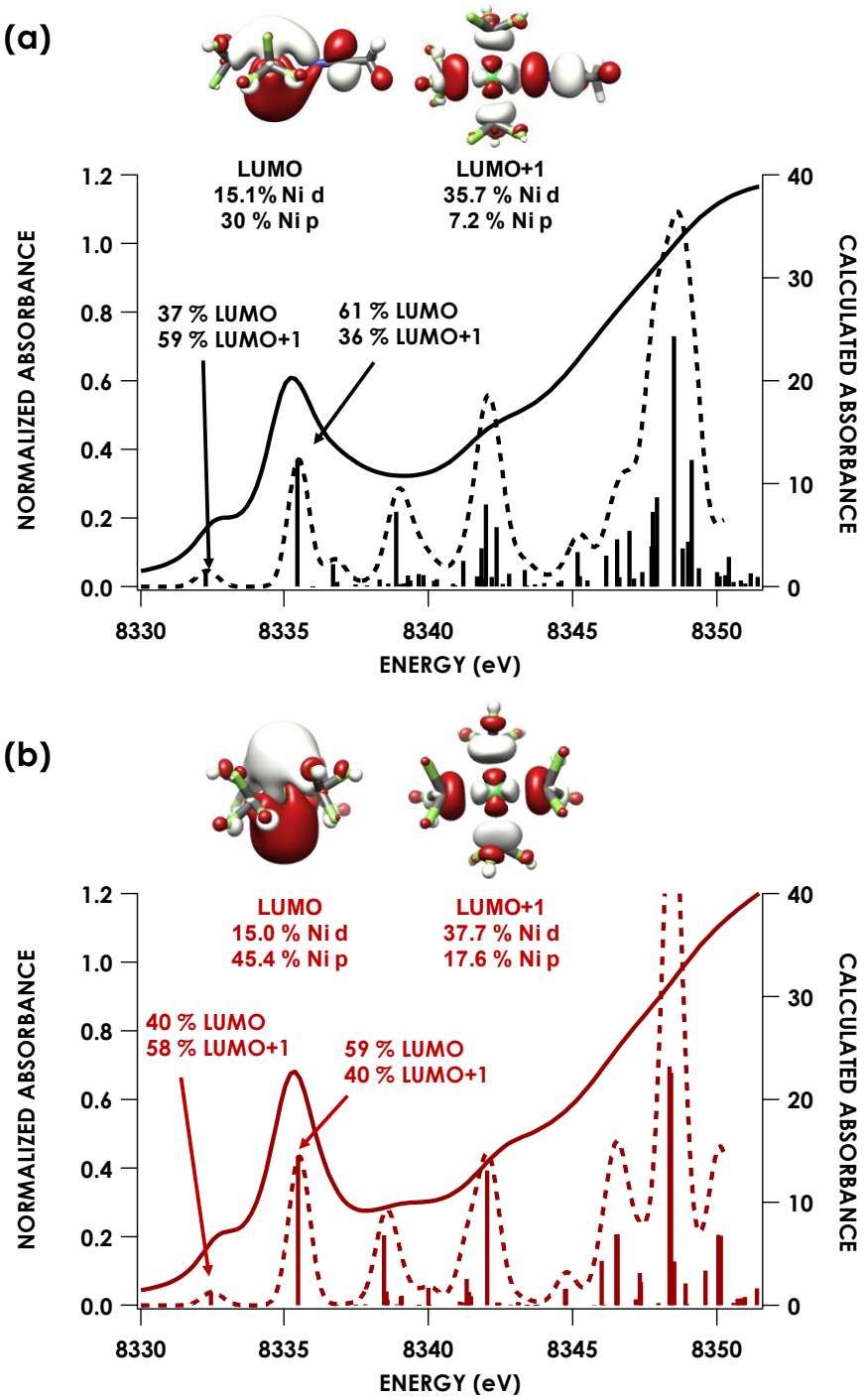


**Figure 6.** Ni K-edge experimental (solid) and computational (dotted) spectra for **5** (a) and **6** (b). TDDFT orbital contributions to pre-edge transitions are shown as well as orbital composition of the LUMO and LUMO+1 orbitals. Calculations were performed using a hybrid density functional theory calculation (B3LYP, ZORA-def2-TZVP(-f) on all atoms, with CP(PPP) on Ni). Orbitals are plotted at isovalues of 0.03 au.

Spectroscopy-oriented configuration interaction (SORCI) calculations,[32] which account for the possibility of multiconfigurational ground states and dynamical electron correlation were also carried out to interrogate the electronic structures of **5** and **6**. These calculations were based on complete active space references with 16 electrons distributed among 10 orbitals (CAS 16,10). The ground state of each complex is dominated (ca. 85 % in either case) by a single electronic configuration—the ground states are effectively single-configurational. The resulting average atomic natural orbitals (AANOs) are occupied in a manner that is consistent with the expected orbital ordering based on convention and based on the progression of intensities in the K-edge XAS (Figure 7). Frontier Ni 3d hole character is entirely contained within the LUMO, which comprises 54.0 % Ni 3d character in **5** and 52.4 % in **6**, again consistent with the $L_{2,3}$-edge XAS and lending further support to the contention that **5** and **6** are highly covalent complexes exhibiting effectively $d^9$ electronic configurations. The calculated UV/vis absorption spectra agree well with the experimental data. The ca. 350 nm absorption bands are predicted as HOMO $\rightarrow$ LUMO transitions (Figure 8). Given the high degree of metal character in the participating orbitals, these transitions can reasonably be assigned as predominantly d-d in nature as suggested by their moderately low extinction coefficients.

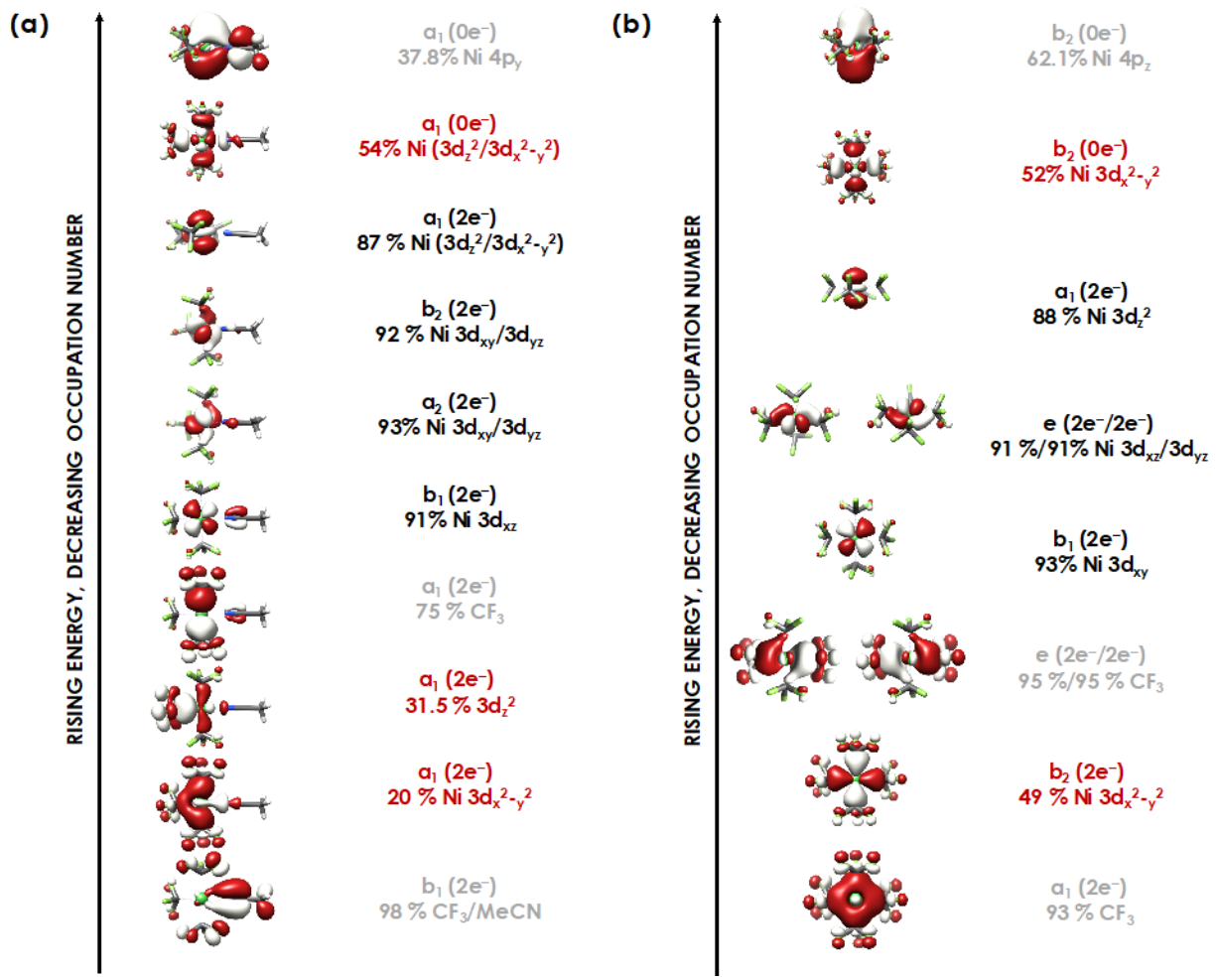


**Figure 7.** Average atomic natural orbitals (AANOs) for **5** (a) and **6** (b) generated from a SORCI calculation employing a 16-electron, 10-orbital active space. Orbitals are labeled assuming $C_{2v}$ symmetry for **5** and $D_{2d}$ symmetry for **6**. Metal dominated orbitals are shown in black, ligand dominated atomic orbitals are shown in grey and orbitals with significant mixing between ligand and metal are shown in red. Calculations were initiated by using a starting set of orbitals generated through a hybrid density functional theory calculation (B3LYP, ZORA-def2-TZVP(-f) on all atoms, with CP(PPP) on Ni). Orbitals are plotted at isovalues of 0.03 au.

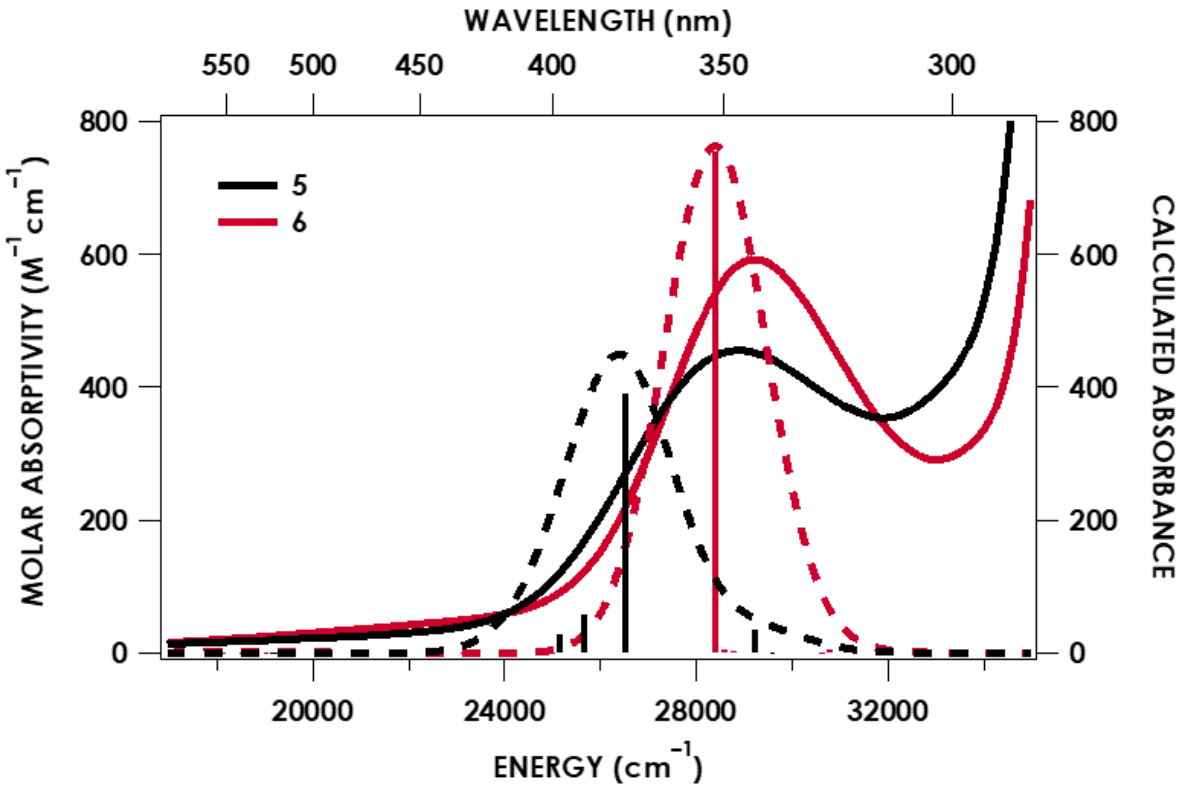


**Figure 8.** Room-temperature UV/visible absorption spectra (solid) of compounds **5** and **6** overlaid with SORCI-calculated UV/vis absorption spectra (dotted). The dominant contribution to each the ca. 350 nm bands in each case is predicted to be the HOMO to LUMO excitation.

*Reactivity.*

The knowledge that monoanionic **5** can accommodate an additional trifluoromethyl anion to afford **6** prompted us to explore the reactivity of **5** with a different nucleophile to determine if a heteroleptic dianionic complex could be prepared. If so, such structures could potentially be developed as intermediates in new nickel-mediated trifluoromethylations, akin to the emerging methodologies involving $[Cu(CF_3)_3(R)]^-$. Reaction of **5** with [PhO][$NMe_4$] indeed led to the production of the new dianionic nickel phenoxide complex **7**. The solubility properties of **7** bearing pure phosphonium counter-ions enable its selective precipitation (80% based on available $PPh_4$ counter-ion) as an analytically pure and crystalline solid, and the ORTEP diagram of **7** is shown in Figure 1. Interestingly, NMR data suggests that when isolated crystals of **7** are dissolved in MeCN, the phenolate moiety dissociates from nickel and reaffords monoanionic complex **5** in solution (eq 1). Benzene is generated in the process along with

triphenylphosphine oxide, indicating a non-innocent interaction between phenoxide and the phosphonium counter-ion. Equilibrium processes between phosphonium salts and phenoxide-derived phosphoranes is known[33] but to our knowledge these interactions leading to the irreversible generation of phosphine oxide is unknown. Control experiments show that simple reaction of $[NMe_4][OPh]$ with $[PPh_4Cl]$ in acetonitrile solvent in the absence of nickel indeed leads to $[O{=}PPh_3]$ plus benzene (see Supporting Information). The source of the oxygen atom does not appear to be derived from the phenoxide moiety, as reaction of $[NMe_4]$[*p*-fluorophenoxide] with $[PPh_4Cl]$ in acetonitrile still yields triphenylphosphine oxide but does not produce any detectable fluorobenzene. Thus, we suspect that adventitious water may be the source of the oxygen atom in $[O{=}PPh_3]$. Changing the counter-ion and reacting $[(MeCN)Ni(CF_3)_3][NBu_4]$ with $[PhO][NMe_4]$ gratifyingly leads to a solution stable complex whose $^{19}F$ NMR signals ($CD_3CN$, δ –21.2 (septet, *J* = 4.1 Hz) and –31.3 (quartet, *J* = 4.1 Hz)) are consistent with the desired $[(PhO)Ni(CF_3)_3][NR_4]$ product. With knowledge of this noninnocent interaction of $[PPh_4]$ with phenoxide, it is clear that judicious choice of counter-ions will be a critical component to methods development with these ligandless complexes of nickel. We are currently working to identify conditions that favor coordination of other organic nucleophiles to **5** to identify redox agents that could ultimately trigger new trifluoromethyl cross-couplings at ligandless nickel.

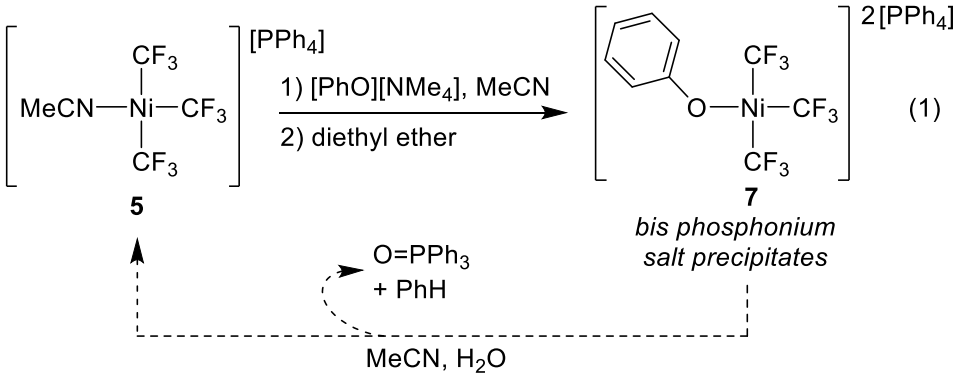


Preliminary explorations of the reactivities of **5** and **6** are described in equations 2 and 3. Complex **5** reacts with the two electron oxidant bis(4-tert-butylphenyl)iodonium hexafluorophosphate to afford trifluoromethylated arene in 54% yield, producing $[(MeCN)_2Ni(CF_3)_2]$ (**4**) in 75% yield as the only detectable nickel containing product (eq 2). Hypervalent iodine reagents are known to oxidize both Pd(II) and Ni(II) to Pd(IV) and Ni(IV),[34] so we speculate that the intermediate in this trifluoromethylation reaction is the high valent $[Ar–Ni^{IV}(CF_3)_3(MeCN)_2]$. Such a species, upon reductive elimination or aryl–$CF_3$ product would afford **4** as the nickel-containing byproduct. Further experiments with **6** shows that

oxidation to unsupported and formally nickel(IV) trifluoromethyl derivatives is indeed possible (eq 3). We observed that a two electron oxidation of **6** with potassium persulfate produced a new species detected by $^{19}F$ NMR spectroscopy ($CD_3CN$, δ -19.15 (sept, *J* = 7.3 Hz) and -30.60 (sept, *J* = 7.3 Hz) in 11% NMR yield along with other fluorine-containing nickel species consistent with $[(SO_4)Ni(CF_3)_2(MeCN)_2]$, $[Ni(CF_3)_4(MeCN)_2]$, and $[Ni(CF_3)_5]^-$ (see Supporting Information). Fortuitous crystallization of one of the new species from MeCN/ether enabled its solid-state structure determination (Figure 9) and confirms the identity of the crystallized compound as $[Ni(CF_3)_4(SO_4)][PPh_4]_2$ (**8**, eq 3). To our knowledge, this is the first example of an unsupported trifluoromethyl nickel(IV) complex, and the identification of such a structure lends credence to the proposal that a high-valent nickel(IV) species is a viable intermediate in the trifluoromethylation reaction described in equation 2. Further efforts to develop trifluoromethylation chemistry with **5** and **6** are planned in our laboratories.

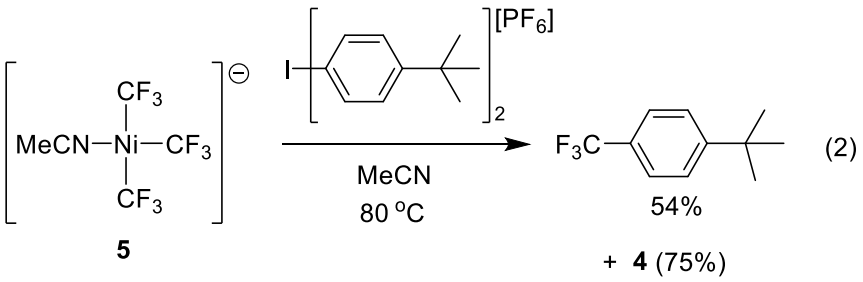


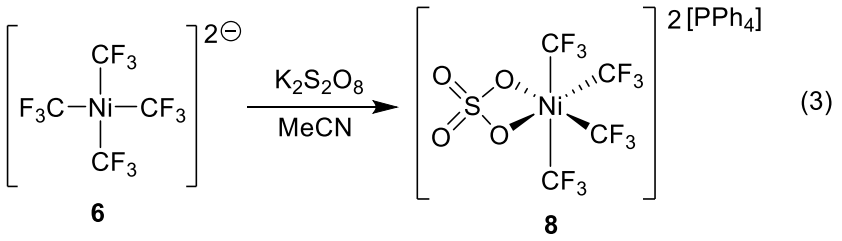

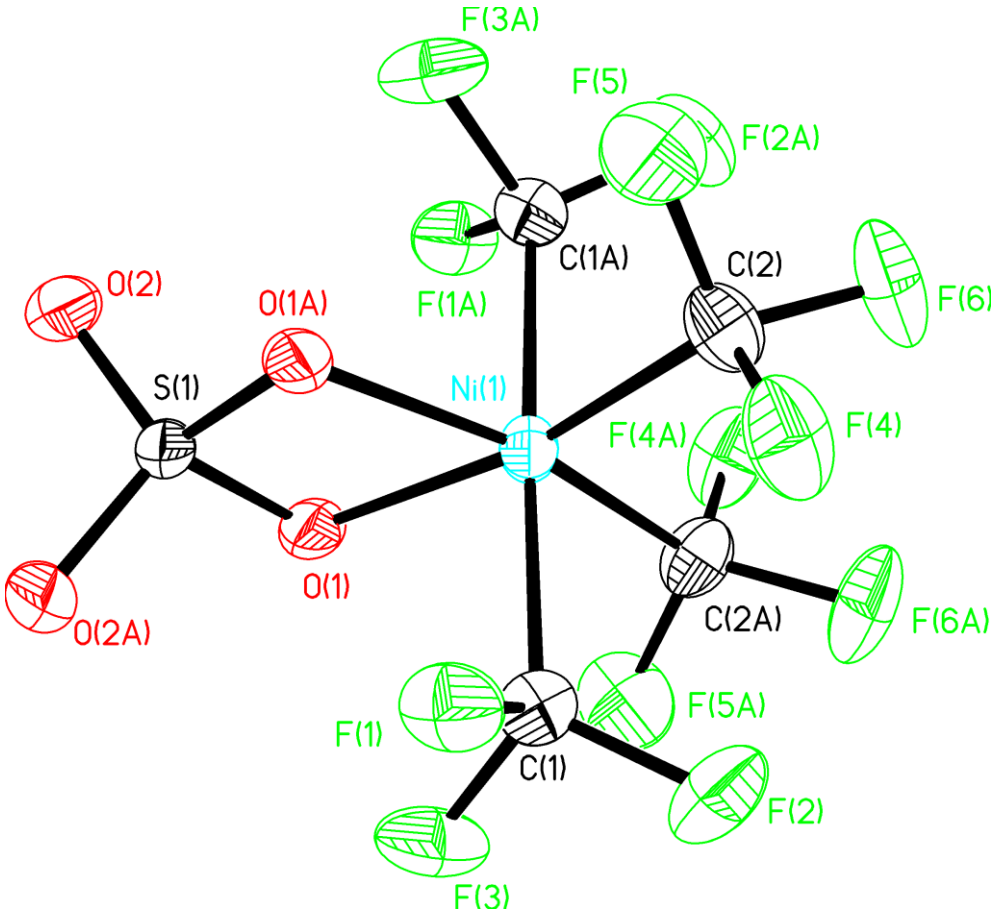


**Figure 9.** ORTEP diagram of **8**. Selected bond lengths (Å): Ni1-C1 2.021(6); Ni1-C2 1.942(6); Ni1-O1 1.964(4); Selected bond angles (°): C2-Ni1-C2A 97.7(4); C2-Ni1-O1 94.7(2); O1-Ni1-O1A 73.0(3); C2-Ni1-C1 92.0(3); C1-Ni1-C1A 177.9(3); O1-S1-O1A 99.5(3).

**Conclusions**

Herein we describe easy access to $[(MeCN)Ni(CF_3)_3]^-$ and $[Ni(CF_3)_4]^{2-}$ and provide full experimental and computational analyses of their electronic structures. The trifluoromethyl ligands, by virtue of their highly covalent interactions with nickel, render both **5** and **6** to physically more reduced states than their formal oxidation state implies. Spectroscopic data and electronic structure calculations support ground state $d^9$ electronic configurations for both $[(MeCN)Ni(CF_3)_3]^-$ and $[Ni(CF_3)_4]^{2-}$, and surprisingly show that holes can be distributed on trifluoromethyl ligands even in nickel complexes bearing formally common oxidation states. The cyclic voltammetry studies show that oxidations of $[(MeCN)Ni(CF_3)_3]^-$ and

$[Ni(CF_3)_4]^{2-}$ are facile, which bodes well for the development of redox-triggered methodologies at nickel. As copper exhibits relatively weak backbonding towards pi-acceptors,[35-36] the nickel complexes **5** and **6** may show broader applicability than **1**-**3** in emergent synthetic methods involving pi-systems of organic substrates. Finally, two important precedents regarding the reactivity of the unsupported complexes **5** and **6** have been set in this report. We have shown that **5** reacts with a bis(aryl)iodonium salt to afford a trifluoromethylated arene, indicating the viability the unsupported complexes in important C-C bond forming reactions. Moreover, the clean formation of **4** as the byproduct of the trifluoromethylation reaction bodes well for future development of catalytic processes. We have also established that the ligandless precursor **6** can be used to directly prepare a formally Ni(IV) complex, showing for the first time that supporting ligands are not a requirement for accessing the higher valent states of trifluoromethyl nickel.

**ASSOCIATED CONTENT**

**Supporting Information Available:** Crystallographic information files (CIF) and NMR spectral data. This material is available free of charge via the internet at http://pubs.acs.org.

**Corresponding author:** *D. A. V.: fax, 1-610-758-6536. E-mail: vicic@lehigh.edu.
ORCID
David A. Vicic: 0000-0002-4990-0355
Scott T. Shreiber: 0000-0002-4224-7461
Mikhail N. Khrizanforov: 0000-0003-4714-4143
Yulia H. Budnikova: 0000-0001-9497-4006
Yulia B. Dudkina: 0000-0003-2830-0438

**Notes:** The authors declare no competing financial interests

**Acknowledgements:** D.A.V. thanks the Office of Basic Energy Sciences of the U. S. Department of Energy (DE-SC0009363) for support of this work. K.M.L. thanks the National Science Foundation (CHE-1454455) for support. XAS data were obtained at SSRL, which is supported by the U.S. Department of Energy, Office of Science, Office of Basic Energy Sciences under Contract No. DE-AC02-76SF00515. The SSRL Structural Molecular Biology Program is supported by the Department of Energy's Office of Biological and Environmental Research, and by NIH/HIGMS (including P41GM103393). The work at SSRL was also supported by the U.S. Department of Energy Office of Basic Energy Sciences proposal No. 100487.

**Accession Codes**

CCDC 1981245-1981247 and 1988483 contain the supplementary crystallographic data for this paper. These data can be obtained free of charge via www.ccdc.cam.ac.uk/data_request/cif, or by e-mailing data_request@ccdc.cam.ac.uk, or by contacting The Cambridge Crystallographic Data Centre, 12 Union Road, Cambridge CB2 1EZ, UK; fax: +44 1223 336033.

**References:**


1. Willert-Porada, M. A.; Burton, D. J.; Baenziger, N. C., Synthesis and x-ray structure of bis(trifluoromethyl)(N,N-diethyldithiocarbamato)copper; a remarkably stable perfluoroalkylcopper(III) complex. *J. Chem. Soc., Chem. Commun.* **1989,** (21), 1633-4.
2. Naumann, D.; Roy, T.; Tebbe, K. F.; Crump, W., Synthesis and structure of a surprisingly stable tetrakis(trifluoromethyl)cuprate(III) salt. *Angew. Chem.* **1993,** *105*, 1555-6.
3. Hoffmann, R.; Alvarez, S.; Mealli, C.; Falceto, A.; Cahill, T. J.; Zeng, T.; Manca, G., From Widely Accepted Concepts in Coordination Chemistry to Inverted Ligand Fields. *Chem. Rev.* **2016,** *116*, 8173-8192.
4. Steen, J. S.; Knizia, G.; Klein, J. E. M. N., σ-Noninnocence: Masked Phenyl-Cation Transfer at Formal NiIV. *Angew. Chem., Int. Ed.* **2019,** *58*, 13133-13139.
5. Snyder, J. P., Elusiveness of CuIII complexation; preference for trifluoromethyl oxidation in the formation of [CuI(CF3)4]- salts. *Angew. Chem., Int. Ed. Engl.* **1995,** *34* (1), 80-1.
6. Kaupp, M.; von Schnering, H. G., Formal Oxidation State versus Partial Charge—A Comment. *Angew. Chem. Int. Ed.* **1995,** *34*, 986-986.
7. Alvarez, S.; Hoffmann, R.; Mealli, C., A Bonding Quandary—or—A Demonstration of the Fact That Scientists Are Not Born With Logic. *Chem. – Eur. J.* **2009,** *15*, 8358-8373.
8. Walroth, R. C.; Lukens, J. T.; MacMillan, S. N.; Finkelstein, K. D.; Lancaster, K. M., Spectroscopic Evidence for a $3d^{10}$ Ground State Electronic Configuration and Ligand Field Inversion in $[Cu(CF_3)_4]^{1-}$ *J. Am. Chem. Soc.* **2016,** *138*, 1922-1931.
9. Gao, C.; Macetti, G.; Overgaard, J., Experimental X-ray Electron Density Study of Atomic Charges, Oxidation States, and Inverted Ligand Field in $Cu(CF_3)_4^-$ *Inorg. Chem.* **2019,** *58*, 2133-2139.
10. DiMucci, I. M.; Lukens, J. T.; Chatterjee, S.; Carsch, K. M.; Titus, C. J.; Lee, S. J.; Nordlund, D.; Betley, T. A.; MacMillan, S. N.; Lancaster, K. M., The Myth of $d^8$ Copper(III). *J. Amer. Chem. Soc.* **2019,** *141*, 18508-18520.
11. Zhang, S.-L.; Bie, W.-F., Ligand-dependent formation of ion-pair CuI/CuIII trifluoromethyl complexes containing bisphosphines. *Dalton Trans.* **2016,** *45*, 17588-17592.
12. Baya, M.; Joven-Sancho, D.; Alonso, P. J.; Orduna, J.; Menjón, B., M−C Bond Homolysis in Coinage-Metal $[M(CF_3)_4]^-$ Derivatives. *Angew. Chem.* **2019,** *131*, 10059-10063.
13. Tan, X.; Liu, Z.; Shen, H.; Zhang, P.; Zhang, Z.; Li, C., Silver-Catalyzed Decarboxylative Trifluoromethylation of Aliphatic Carboxylic Acids. *J. Am. Chem. Soc.* **2017,** *139*, 12430-12433.
14. Lu, Z.; Liu, H.; Liu, S.; Leng, X.; Lan, Y.; Shen, Q., A Key Intermediate in Copper-Mediated Arene Trifluoromethylation, $[nBu_4N][Cu(Ar)(CF_3)_3]$: Synthesis, Characterization, and $C(sp^2)–CF_3$ Reductive Elimination. *Angew. Chem. Int. Ed.* **2019,** *58*, 8510-8514.

15. Paeth, M.; Carson, W.; Luo, J.-H.; Tierney, D.; Cao, Z.; Cheng, M.-J.; Liu, W., Copper-Mediated Trifluoromethylation of Benzylic $Csp^3$–H Bonds. *Chem. – Eur. J.* **2018,** *24*, 11559-11563.
16. Guo, S.; AbuSalim, D. I.; Cook, S. P., 1,2-(Bis)trifluoromethylation of Alkynes: A One-Step Reaction to Install an Underutilized Functional Group. *Angew.Chem. Int. Ed.* **2019,** *58*, 11704-11708.
17. Guo, S.; AbuSalim, D. I.; Cook, S. P., Aqueous Benzylic C-H Trifluoromethylation for Late-Stage Functionalization. *J. Am. Chem. Soc.* **2018,** *140*, 12378-12382.
18. Zhang, S.-L.; Bie, W.-F., Isolation and characterization of copper(III) trifluoromethyl complexes and reactivity studies of aerobic trifluoromethylation of arylboronic acids. *RSC Adv.* **2016,** *6*, 70902-70906.
19. Yu, S.; Dudkina, Y.; Wang, H.; Kholin, K. V.; Kadirov, M. K.; Budnikova, Y. H.; Vicic, D. A., Accessing perfluoroalkyl nickel(ii), (iii), and (iv) complexes bearing a readily attached [$C_4F_8$] ligand. *Dalton Trans.* **2015,** *44*, 19443-19446.
20. Camasso, N. M.; Sanford, M. S., Design, synthesis, and carbon-heteroatom coupling reactions of organometallic nickel(IV) complexes. *Science* **2015,** *347*, 1218-1220.
21. Chong, E.; Kampf, J. W.; Ariafard, A.; Canty, A. J.; Sanford, M. S., Oxidatively Induced C–H Activation at High Valent Nickel. *J. Am. Chem. Soc.* **2017,** *139*, 6058-6061.
22. Bour, J. R.; Ferguson, D. M.; McClain, E. J.; Kampf, J. W.; Sanford, M. S., Connecting Organometallic Ni(III) and Ni(IV): Reactions of Carbon-Centered Radicals with High-Valent Organonickel Complexes. *J. Am. Chem. Soc.* **2019,** *141*, 8914-8920.
23. Zhang, C.-P.; Wang, H.; Klein, A.; Biewer, C.; Stirnat, K.; Yamaguchi, Y.; Xu, L.; Gomez-Benitez, V.; Vicic, D. A., A Five-Coordinate Nickel(II) Fluoroalkyl Complex as a Precursor to a Spectroscopically Detectable Ni(III) Species. *J. Am. Chem. Soc.* **2013,** *135*, 8141-8144.
24. Shearer, J.; Dehestani, A.; Abanda, F., Probing Variable Amine/Amide Ligation in $Ni^{II}N_2S_2$ Complexes Using Sulfur K-Edge and Nickel L-Edge X-ray Absorption Spectroscopies: Implications for the Active Site of Nickel Superoxide Dismutase. *Inorg. Chem.* **2008,** *47*, 2649-2660.
25. Koroidov, S.; Hong, K.; Kjaer, K. S.; Li, L.; Kunnus, K.; Reinhard, M.; Hartsock, R. W.; Amit, D.; Eisenberg, R.; Pemmaraju, C. D.; Gaffney, K. J.; Cordones, A. A., Probing the Electron Accepting Orbitals of Ni-Centered Hydrogen Evolution Catalysts with Noninnocent Ligands by Ni L-Edge and S K-Edge X-ray Absorption. *Inorg. Chem.* **2018,** *57*, 13167-13175.
26. Eisebitt, S.; Böske, T.; Rubensson, J. E.; Eberhardt, W., Determination of absorption coefficients for concentrated samples by fluorescence detection. *Phys. Rev. B* **1993,** *47*, 14103-14109.
27. B.L. Henke, E.M. Gullikson, and J.C. Davis. *X-ray interactions: photoabsorption, scattering, transmission, and reflection at E=50-30000 eV, Z=1-92*, Atomic Data and Nuclear Data Tables Vol. **54** (no.2), 181-342 (July 1993).
28. Golnak, R.; Xiao, J.; Atak, K.; Unger, I.; Seidel, R.; Winter, B.; Aziz, E. F., Undistorted X-ray Absorption Spectroscopy Using s-Core-Orbital Emissions. *J. Phys. Chem. A* **2016,** *120*, 2808-2814.
29. Sarangi, R.; DeBeer George, S.; Rudd, D. J.; Szilagyi, R. K.; Ribas, X.; Rovira, C.; Almeida, M.; Hodgson, K. O.; Hedman, B.; Solomon, E. I., Sulfur K-Edge X-ray Absorption Spectroscopy as a Probe of Ligand−Metal Bond Covalency: Metal vs Ligand Oxidation in Copper and Nickel Dithiolene Complexes. *J. Am. Chem. Soc.* **2007,** *129*, 2316-2326.
30. Solomon, E. I.; Hedman, B.; Hodgson, K. O.; Dey, A.; Szilagyi, R. K., Ligand K-edge X-ray absorption spectroscopy: covalency of ligand–metal bonds. *Coord. Chem. Rev.* **2005,** *249*, 97-129.
31. DeBeer George, S.; Petrenko, T.; Neese, F., Prediction of Iron K-Edge Absorption Spectra Using Time-Dependent Density Functional Theory. *J. Phys. Chem. A* **2008,** *112*, 12936-12943.
32. Neese, F., A spectroscopy oriented configuration interaction procedure. *J. Chem. Phys.* **2003,** *119*, 9428-9443.

33. Sigal, I. S.; Westheimer, F. H., Disproportionation among aryloxyphosphoranes. *J. Am. Chem. Soc.* **1979,** *101*, 5329-34.
34. Sousa e Silva, C. F.; Tierno, F. A.; Wengryniuk, E. S., Hypervalent Iodine Reagents in High Valent Transition Metal Chemistry. *Molecules* **2017,** *22*, 780.
35. Munakata, M.; Kitagawa, S.; Kosome, S.; Asahara, A., Studies of copper(I) olefin complexes. Formation constants of copper olefin complexes with 2,2'-bipyridine, 1,10-phenanthroline, and their derivatives. *Inorg. Chem.* **1986,** *25*, 2622-7.
36. Strauss, S. H., Copper(I) and silver(I) carbonyls. To be or not to be nonclassical. *Dalton* **2000,** 1-6.

For Table of Contents Only: